ADAPTIVE LINE ENHANCEMENT USING A SECOND-ORDER IIR FILTER

H.J.W. Belt, A.C. den Brinker, and F.P.A. Benders

Eindhoven University of Technology, Department of Electrical Engineering
P.O. Box 513, NL-5600 MB EINDHOVEN, The Netherlands
Email: H.J.W.Belt@ele.tue.nl

ABSTRACT

A second-order IIR filter is considered as the basic component of an Adaptive Line enhancer (ALE). As a new feature, the bandwidth of the proposed ALE is adapted simultaneously with the center frequency. This leads to the possibility to combine convergence speed and accuracy. The adaptation of the filter poles is controlled by a sign algorithm. The stepsizes are chosen such that transients caused by the retuning of the filter are ensured to remain much smaller in amplitude than the response of the filter to the input signal. When the input signal consists of a sinusoid corrupted by wide-band noise, an accurate frequency parameter estimate can be obtained with an algorithm given in this paper.

1. THE GENERAL ALE

Separation of a low-level sinusoid or narrow-band signal from broad-band noise is a classical problem in the field of signal processing. In the past a so-called Adaptive Line Enhancer (ALE) has been introduced for this purpose by Widrow *et al.* [1]. The general scheme of the ALE is depicted in Fig. 1. The ALE input $d(k)$ is assumed to be the sum of a narrow-band signal $s(k)$, and a broad-band signal $n(k)$. The parameters of the prediction filter $H_P(z)$ are adapted in such a way that the mean-squared error (mse) $E[\epsilon^2(k)]$ is minimized. The ALE operates by virtue of the difference between the correlation lengths of $s(k)$ and $n(k)$. The delay parameter Δ should be chosen larger than the correlation length of $n(k)$, but smaller than the correlation length of $s(k)$. In this case, it is possible for $H_P(z)$ to make a Δ-step ahead prediction of $s(k-\Delta)$ based on the present and past samples of $d(k-\Delta)$. However, $H_P(z)$ will not be able to predict $n(k)$ from knowledge about present and past samples of $n(k-\Delta)$. As a result, after the parameters of $H_P(z)$ have converged towards their optimal values, the ALE output $y(k)$ is approximately equal to $s(k)$, and the error signal $\epsilon(k)$ is approximately equal to $n(k)$.

2. THE SECOND-ORDER IIR FILTER

Often a transversal filter is used for the prediction filter, e.g. in [1]-[4]. However, the major drawback of a transversal filter is the large number of taps that is required to obtain sharp bandpass characteristics. Recently, much attention has been paid to ALEs based on second-order IIR filters, e.g. in [5]-[10]. An IIR filter is inherently able to show

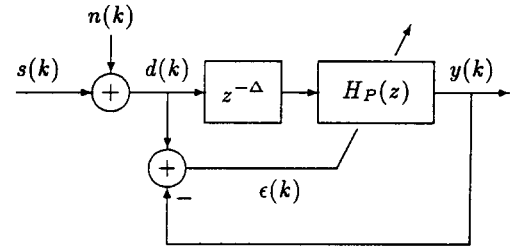

Figure 1: The adaptive line enhancer.

sharp bandpass characteristics with only a few parameters. The second-order IIR filter proposed in this paper is shown in Fig. 2. The filter pole p is given by $p = re^{j\phi}$, where r is the pole radius ($0 < r < 1$), and ϕ is the pole angle ($0 < \phi < \pi$). For r close to but smaller than 1, the pole radius r determines the bandwidth of the prediction filter, and the pole angle ϕ determines the center frequency. The output $y(k)$ of $H_P(z)$ is composed of a weighted sum of $u_1(k)$ and $u_2(k)$. As a consequence of the specific structure of $H_P(z)$, the signals $u_1(k)$ and $u_2(k)$ are orthogonal, meaning that their cross-power $E[u_1(k)u_2(k)]$ is equal to zero.

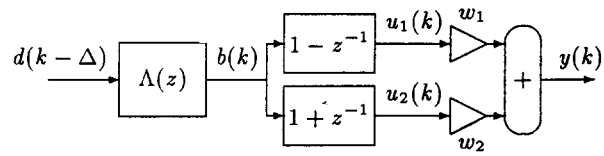

Figure 2: The second-order IIR prediction filter, with $\Lambda(z) = z^2/(z-p)(z-p^*)$.

When we assume that ϕ is not too near the values 0 and π, and r is close to but smaller than 1, then a good approximation of the bandwidth B of $H_P(z)$ is given by $B \approx 2(1-r)$. In the case that the weights and ϕ are optimal in the mse sense, and assuming that ϕ and r satisfy the same assumptions, then the Signal to Noise Improvement Ratio (SNIR) of the ALE can be approximated by SNIR $\approx 1/(1-r)$, see [7].

0-7803-2431-5/95 $4.00 © 1995 IEEE

3. THE ADAPTATION ALGORITHM

Optimization of the weights $\underline{w} = (w_1, w_2)^t$ is a linear problem, since the filter output varies linearly with the weights. Optimization of the filter pole $p = re^{j\phi}$ however, is a non-linear problem. In this section, an adaptation algorithm for both optimization problems is derived. In the analysis it is assumed that the two adaptation processes have totally different time constants, meaning that they operate on a totally different time scale. In this way these processes are approximately independent. This justifies the fact that the adaptation processes are analyzed separately, while they will be performed simultaneously.

3.1. Optimizing the Weights

The optimal weights $\underline{w}_{opt}$ are given by the Wiener-Hopf equations, which read in matrix form $\underline{w}_{opt} = R^{-1}P$. Here, R is the correlation matrix of $\underline{u}(k) = (u_1(k), u_2(k))^t$ and P is the correlation vector between $d(k)$ and $\underline{u}(k)$. Since $u_1(k)$ and $u_2(k)$ are orthogonal, R is only non-zero on the main diagonal. This yields a simple RLS-algorithm to adapt the weights, given by (in the rest of this paper $i = 1, 2$):

$$\hat{R}_{ii}(k) = \theta\hat{R}_{ii}(k-1) + (1-\theta)u_i^2(k), \quad (1)$$

$$\hat{P}_i(k) = \theta\hat{P}_i(k-1) + (1-\theta)u_i(k)d(k), \quad (2)$$

$$\underline{w}(k) = \left(\frac{\hat{P}_1(k)}{\hat{R}_{11}(k)}, \frac{\hat{P}_2(k)}{\hat{R}_{22}(k)}\right)^t. \quad (3)$$

Here, $\hat{}$ stands for an estimate of the corresponding expectation.

3.2. Optimizing the Pole

In the literature, the pole radius r is usually kept constant during the adaptation process. In [7], the bandwidth is varied by increasing r in time towards its final predetermined value. In none of the studies we know of, the pole radius is optimized simultaneously with the pole angle.

A sign algorithm is proposed to adaptively optimize the pole radius r and the cosine of the pole angle $\gamma = \cos\phi$ (we adapt γ instead of ϕ since this simplifies the calculation of a gradient). The motivation for the use of a sign algorithm instead of a gradient-based method is, that the necessary compromise between accuracy and speed is extremely difficult to make using a gradient-based method for the optimization of the recursive parameters of a sharp bandpass filter. Adaptation of the poles inevitably leads to transients at the filter output. The transients are analyzed based on a state space description of $H_p(z)$, see the Appendix. This analysis yields stepsizes for r and γ that guarantee the transients to remain small compared to the filter response to the input signal. We arrive at the following optimization algorithm:

$$r(k+1) = r(k) - \mu_r(k)\ \mathrm{sign}\left(\epsilon(k)\frac{\partial\epsilon(k)}{\partial r}\right), \quad (4)$$

$$\gamma(k+1) = \gamma(k) - \mu_\gamma(k)\ \mathrm{sign}\left(\epsilon(k)\frac{\partial\epsilon(k)}{\partial\gamma}\right), \quad (5)$$

with the stepsizes given by

$$\mu_r(k) = c_r(1-r(k))^2, \quad (6)$$

$$\mu_\gamma(k) = c_\gamma(1-r(k))^2\sin\phi(k). \quad (7)$$

Here, c_r and c_γ are small constants satisfying $c_r, c_\gamma \ll \frac{1}{2}\sqrt{2}$. As an added advantage of the chosen algorithm, the poles are ensured to remain within the unit circle, and thus the filter remains always stable. If no *a priori* knowledge about the frequency contents of $s(k)$ is known, then, initially, the pole is put on the imaginary axis ($\phi = \pi/2$) for reasons of symmetry. This initial pole is given a small radius for two reasons [7]. First, because with no *a priori* knowledge about the frequency contents of $s(k)$, a large bandwidth is desired to ensure that $H_P(z)$ "senses" $s(k)$. Second, at the beginning of the adaptation process a short "memory" of the filter is desired to ensure that the incorrect initial states of $H_P(z)$ are "forgotten" soon.

The concept of the totally different time scales (the weights adapt must faster than the pole) of the two adaptation algorithms justifies the fact that in the following analysis $\underline{w} = \underline{w}_{opt}$ is used. The gradients $\partial\epsilon(k)/\partial r$ and $\partial\epsilon(k)/\partial\gamma$ are obtained by (in the rest of this paper $\chi = r, \gamma$)

$$\frac{\partial\epsilon(k)}{\partial\chi} = -\underline{w}_{opt}^t\frac{\partial\underline{u}(k)}{\partial\chi} - \underline{u}^t(k)\frac{\partial\underline{w}_{opt}}{\partial\chi}. \quad (8)$$

With reference to Fig. 2, we define $U_1(z)$, $U_2(z)$ and $B(z)$ as the z-transforms of $u_1(k)$, $u_2(k)$ and $b(k)$, respectively. Then, the gradients $\partial\underline{u}(k)/\partial\chi$ can be obtained as the inverse z-transforms of

$$\frac{\partial U_i(z)}{\partial\gamma} = 2rz^{-1}\Lambda(z)\left(1 + (-1)^i z^{-1}\right)B(z), \quad (9)$$

$$\frac{\partial U_i(z)}{\partial r} = \frac{1}{r}\left(\gamma - rz^{-1}\right)\frac{\partial U_i(z)}{\partial\gamma}. \quad (10)$$

Using the Wiener-Hopf equations, we obtain for the derivatives of the optimal weights with respect to the pole parameters

$$\frac{\partial w_{opt,i}}{\partial\chi} = \frac{\partial}{\partial\chi}\left\{\frac{P_i}{R_{ii}}\right\} = \frac{1}{R_{ii}}\left\{\frac{\partial P_i}{\partial\chi} - w_{opt,i}\frac{\partial R_{ii}}{\partial\chi}\right\}. \quad (11)$$

The derivatives $\partial P_i/\partial\chi$ and $\partial R_{ii}/\partial\chi$ at sample moment k can be estimated recursively as follows

$$\frac{\partial\hat{P}_i(k)}{\partial\chi} = \theta\frac{\partial\hat{P}_i(k-1)}{\partial\chi} + (1-\theta)d(k)\frac{\partial u_i(k)}{\partial\chi}, \quad (12)$$

$$\frac{\partial\hat{R}_{ii}(k)}{\partial\chi} = \theta\frac{\partial\hat{R}_{ii}(k-1)}{\partial\chi} + 2(1-\theta)u_i(k)\frac{\partial u_i(k)}{\partial\chi}. \quad (13)$$

Now the adaptation algorithm for the pole radius and angle is given by (4)-(13).

4. A FREQUENCY ESTIMATE

In the case that $s(k)$ is a single sinusoid, an instantaneous estimate of its frequency Ω_0 is sometimes desirable. The pole angle $\phi(k)$ can always be used for this purpose. A more accurate frequency estimate can be obtained from the two zeros on the unit circle of the notch transfer $H(z)$ from

$d(k)$ to $\epsilon(k)$. The numerator $N_H(z)$ of $H(z)$ is a polynomial in z of degree $\Delta+1$, and for $\Delta = 1$ its roots can explicitly be determined. For larger values of Δ, an iterative procedure must be used. As an estimate of Ω_0, we will calculate the frequency ω at which $|N_H(e^{j\omega})|^2$ is minimal. At the minimum of $|N_H(e^{j\omega})|^2$, its derivative w.r.t. ω must be equal to zero. The following notation is used:

$$\left.\frac{\partial^i |N_H(e^{j\omega})|^2}{\partial \omega^i}\right|_{\omega=\omega(k)} = N_H^{(i)}(k). \qquad (14)$$

These derivatives can explicitly be derived from $|N_H(e^{j\omega})|^2$. By using a first-order Taylor series approximation of $N_H^{(1)}(k)$ centered on $\omega(k-1)$, we obtain

$$N_H^{(1)}(k) \approx N_H^{(1)}(k-1) + \{\omega(k) - \omega(k-1)\} N_H^{(2)}(k-1) = 0. \qquad (15)$$

An instantaneous estimate for Ω_0 at sample moment k is thus given by

$$\omega(k) = \omega(k-1) - \frac{N_H^{(1)}(k-1)}{N_H^{(2)}(k-1)}. \qquad (16)$$

Initially, we take $\omega(0) = \phi(0)$. To avoid problems with local minima, the calculated frequency estimate is restricted to lie within the prediction filter bandwidth B. Therefore, in the case that $|\omega(k) - \phi(k)| > 1 - r(k)$, we reset $\omega(k)$ to $\phi(k)$.

5. EXPERIMENTAL RESULTS

The results of a single run of the first experiment are shown in Fig. 4. The ALE input signal consists of a sinusoid with frequency 0.5 and amplitude 1, corrupted by zero-mean, white noise ($\sigma_n^2 = 1$). We take $\Delta = 10$, $\theta = 0.99$, and $c_r = c_\gamma = 0.01$. Initially the pole is put on the imaginary axis ($\phi(0) = \pi/2$) for reasons of symmetry, and we take $r(0) = 0.42$. Fig. 4A shows that after 3000 samples a good frequency estimate is obtained. We notice from Fig. 4B that the pole radius increases towards 1, in this way increasing the SNIR. We also notice that the stepsizes become smaller when r becomes larger, in this way increasing the accuracy.

In Fig. 5 the results of a frequency tracking experiment are shown. Apart from the frequency of the sinusoid, all other parameters have been taken the same as in the first experiment. As can be seen from Fig. 5A, the frequency estimate can track the rapid frequency changes very well. Naturally, if desired, these data can always be filtered to obtain a smoother frequency estimate. The pole angle is not capable to track the rapid changes in the frequency. Instead, it converges towards an average frequency. In Fig. 5B, the pole radius converges towards a certain value such that the fluctuations of the frequency Ω_0 remain just within the filter bandwidth.

6. DISCUSSION

In this paper a second-order IIR filter has been considered as the basic component of an ALE. Two separate optimization algorithms have been derived, namely for the poles and for two weights. During operation of the ALE, both algorithms are performed simultaneously. It has been argued that these two algorithms may still be analyzed independently, since they are performed at totally different time scales. The pole radius and angle are both adapted using a sign algorithm. This sign algorithm ensures that the cumulative transient caused by the permanent retuning of the recursive parameters of the filter remains much smaller in amplitude than the filter response to its input signal. The results of two experiments have been shown, illustrating the convergence behaviour and the frequency tracking behaviour of the ALE. It has been shown that fast frequency tracking is possible due to the capability of the weights to rapidly adjust the zeros on the unit circle of the notch filter transfer. The bandwidth of the IIR filter is automatically adjusted to the bandwidth of the undisturbed input signal.

7. APPENDIX

The second-order section $\Lambda(z)$ can be implemented using the direct form 2, as is shown in Fig. 3. Here, $x_1(k)$ and $x_2(k)$ are the internal states, and $d'(k) = d(k-\Delta)$. When r and ϕ are updated, then errors Δx_1 and Δx_2 in the states are introduced. These state errors cause a transient at the output due to the recursive nature of the filter. This transient is now analyzed, assuming that the filter is highly resonant (r close to 1) around the frequency of the input sinusoid ($\phi = \Omega_0$). Therefore, the state errors are mainly determined by the sinusoidal component in $d'(k)$ and we may neglect the noise component. In the following transient analysis we take $d'(k) = A_0 e^{j(\phi k + \psi)}$, with $A_0 \in \mathbb{R}_+$ and ψ a random variable uniformly distributed on the interval $[0, 2\pi)$.

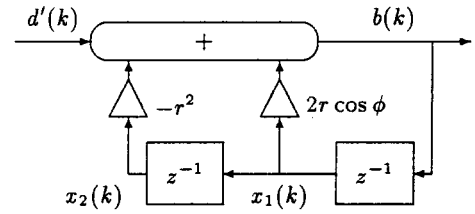

Figure 3: $\Lambda(z)$ implemented in the direct form 2

We consider the transfers $\Lambda_1(z)$ and $\Lambda_2(z)$ from $d'(k)$ to $x_1(k)$ and $x_2(k)$, respectively. The state errors are caused by the changes Δr and $\Delta\phi$ in r and ϕ according to

$$\Delta x_i = -\mathrm{Re}\left\{\left[\Delta\phi \frac{\partial \Lambda_i(z)}{\partial \phi} + \Delta r \frac{\partial \Lambda_i(z)}{\partial r}\right]_{z=e^{j\phi}} A_0 e^{j\psi}\right\}. \qquad (17)$$

The state errors Δx_1 and Δx_2 are the initial conditions $t(-1)$ and $t(-2)$ for the transient $t(k)$, $k = 0, 1, \cdots$. At each iteration step a new transient is introduced. We require that this total transient is much smaller than the filter response to $d'(k)$. Further analysis yields for the upper bound of the relative transient

$$\frac{\sum_{k=0}^{\infty} |t(k)|}{A_0 |\Lambda(e^{j\phi})|} \leq \frac{r}{(1-r)^2} \sqrt{(\Delta r)^2 + (r\Delta\phi)^2}. \qquad (18)$$

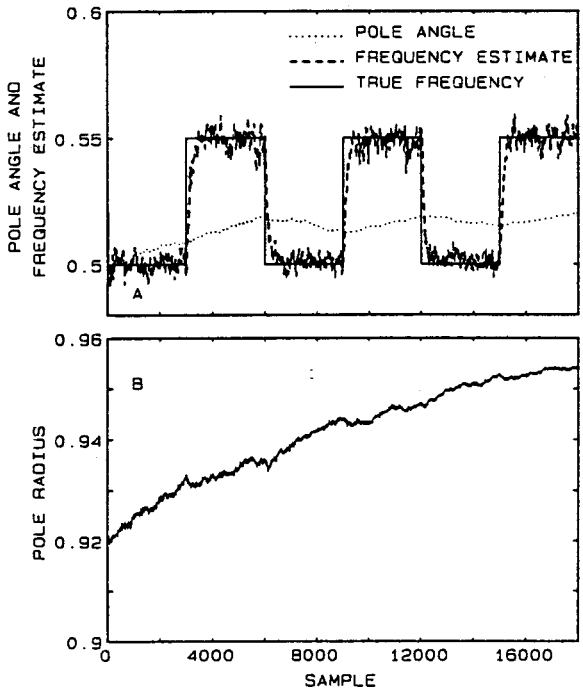

Figure 4: The convergence behaviour of the ALE parameters. A. The pole angle and frequency estimate; B. The pole radius.

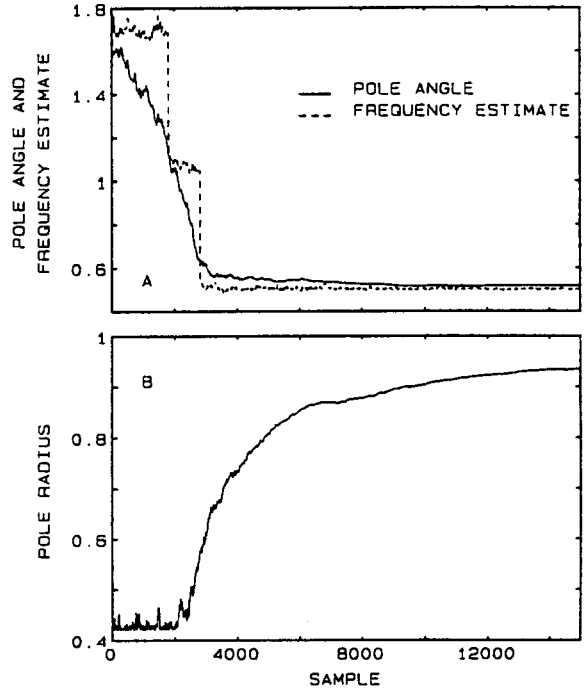

Figure 5: The tracking behaviour of the ALE parameters. A. The pole angle and frequency estimate; B. The pole radius.

By requiring that the right-hand side of (18) is much smaller than 1, the total transient is guaranteed to remain much smaller than the response to $d'(k)$. Therefore, we choose Δr and $\Delta\phi$ to be equal to $c_r(1-r)^2$ and $c_\phi(1-r)^2$, respectively, with $c_r, c_\phi \ll \frac{1}{2}\sqrt{2}$. Since we update $\gamma = \cos\phi$ instead of ϕ we use $\Delta\gamma = c_\gamma(1-r)^2 \sin\phi(k)$, with $c_\gamma = c_\phi$.

8. REFERENCES

[1] B. Widrow, J.R. Glover, H.M. McCool, J. Kaunitz, C.S. Williams, R.H. Hearn, J.R. Zeidler, E.U. Dong, and R.C. Goodlin, "Adaptive Noise Cancelling: Principles and Applications," Proc. IEEE, vol. 63, pp. 1692-1719, 1975.

[2] L.J. Griffiths, "Rapid Measurement of Digital Instantaneous Frequency," IEEE Trans. Acoust. Speech Signal Processing, vol. ASSP-23, pp. 207-222, 1975.

[3] J.R. Treichler, "Transient and Convergent Behavior of the Adaptive Line Enhancer," IEEE Trans. Acoust. Speech Signal Processing, vol. ASSP-27, pp. 53-62, 1979.

[4] J.R. Zeidler, "Performance Analysis of LMS Adaptive Prediction Filters," Proc. IEEE, vol. 78, pp. 1781-1806, 1990.

[5] B. Friedlander, "Analysis and Performance Evaluation of an Adaptive Notch Filter," IEEE Trans. Inf. Theory, vol. IT-30, pp. 283-295, 1984.

[6] D.V. Bhaskar Rao, S.-Y. Kung, "Adaptive Notch Filtering for the Retrieval of Sinusoids in Noise," IEEE Trans. Acoust. Speech Signal Processing, vol. ASSP-32, pp. 791-802, 1984.

[7] A. Nehorai, "A Minimal Parameter Adaptive Notch Filter With Constrained Poles and Zeros," IEEE Trans. Acoust. Speech Signal Processing, vol. ASSP-33, pp. 983-996, 1985.

[8] R.A. David, S.D. Stearns, and G.R. Elliot, "IIR Algorithms for Adaptive Line Enhancement," Proc. Int. Conf. Acoust. Speech Signal Processing, vol. 1, pp. 17-20, 1983.

[9] D.R. Hush, N. Ahmed, R. David, and S.D. Stearns, "An Adaptive IIR Structure for Sinusoidal Enhancement, Frequency Estimation, and Detection," IEEE Trans. Acoust. Speech Signal Processing, vol. ASSP-34, pp. 1380-1390, 1986.

[10] N.I. Cho, C. Choi and S.U. Lee, "Adaptive Line Enhancement by Using an IIR Lattice Notch Filter," IEEE Trans. Acoust. Speech Signal Processing, vol. ASSP-37, pp. 585-589, 1989.